



1 **Methanethiol, dimethyl sulfide and acetone over biologically 2 productive waters in the SW Pacific Ocean**

3

4 Sarah J. Lawson¹, Cliff S. Law^{2,3}, Mike J. Harvey², Tom G. Bell⁴, Carolyn F. Walker², Warren
5 J. de Bruyn⁵ and Eric S. Saltzman⁶

6 ¹ Commonwealth Scientific and Industrial Research Organisation, Oceans and Atmosphere, Aspendale, Australia

7 ² National Institute of Water and Atmospheric Research, Wellington, New Zealand

8 ³ Dept. Chemistry, University of Otago, Dunedin, New Zealand

9 ⁴ Plymouth Marine Laboratory, Plymouth, UK

10 ⁵ Schmidt College of Science and Technology, Chapman University, Orange, California, CA, USA

11 ⁶ Earth System Science, University of California, Irvine, California, USA

12 *Correspondence to:* Sarah J. Lawson (sarah.lawson@csiro.au)

13 **Abstract**

14 Atmospheric methanethiol (MeSH_a), dimethyl sulfide (DMS_a) and acetone (acetone_a) were measured over
15 biologically productive frontal waters in the remote South West Pacific Ocean in summertime 2012 during the
16 Surface Ocean Aerosol Production (SOAP) voyage. MeSH_a mixing ratios varied from below detection limit (< 10
17 ppt) up to 65 ppt and were 3 - 36% of parallel DMS_a mixing ratios. MeSH_a and DMS_a were correlated over the
18 voyage ($R^2=0.3$, slope = 0.07) with a stronger correlation over a coccolithophore-dominated phytoplankton bloom
19 ($R^2 = 0.5$, slope 0.13). The diurnal cycle for MeSH_a shows similar behaviour to DMS_a with mixing ratios varying
20 by a factor of ~2 according to time of day with the minimum levels of both MeSH_a and DMS_a occurring at around
21 16:00 hrs. A positive flux of MeSH was calculated for 3 different nights and ranged from 3.5 - 5.8 $\mu\text{mol m}^{-2} \text{ day}^{-1}$
22 ¹ corresponding to 14 - 24% of the DMS flux ($\text{MeSH}/(\text{MeSH}+\text{DMS})$). Spearman rank correlations with ocean
23 biogeochemical parameters showed a moderate to strong positive and highly significant relationship between both
24 MeSH_a and DMS_a with seawater DMS (DMS_{sw}), and a moderate correlation with total dimethylsulfoniopropionate
25 (total DMSP). A positive correlation of acetone_a with water temperature and negative correlation with nutrient
26 concentrations is consistent with reports of acetone production in warmer subtropical waters. Positive correlations
27 of acetone_a with cryptophyte and eukaryotic phytoplankton numbers, and high molecular weight sugars and
28 Chromophoric Dissolved Organic Matter (CDOM), suggest an organic source. This work points to a significant
29 ocean source of MeSH , highlighting the need for further studies into the distribution and fate of MeSH , and
30 suggests links between atmospheric acetone levels and biogeochemistry over the mid-latitude ocean.

31 In addition, an intercalibration of DMS_a at ambient levels using three independently calibrated instruments showed
32 ~15-25% higher mixing ratios from an Atmospheric Pressure Ionisation-Chemical Ionisation Mass Spectrometer
33 (mesoCIMS) compared to a Gas Chromatograph with Sulfur Chemiluminescence Detector (GC-SCD) and proton
34 transfer reaction mass spectrometer (PTR-MS). PTR-MS and mesoCIMS showed similar temporal behaviour with
35 differences in ambient mixing ratios likely influenced by the DMS_a gradient above the sea surface.

36 **1 Introduction**

37 Volatile organic compounds (VOC) are ubiquitous in the atmosphere and have a central role in secondary particle
38 and tropospheric ozone formation, as well as controlling the oxidative capacity of the atmosphere. VOCs may
39 also impact air quality and human health, through their role in particle and ozone formation, and direct impacts



1 through exposure. The role of the ocean in the global cycle of several VOCs is becoming increasingly recognised,
2 with recent studies showing that the ocean serves as a major source, sink, or both for many pervasive and climate-
3 active VOCs (Law et al., 2013; Liss and Johnson, 2014; Carpenter and Nightingale, 2015).

4

5 The ocean is a major source of reduced volatile sulfur gases (Lee and Brimblecombe, 2016) and the most well-
6 studied of these is dimethyl sulfide (DMS). Since the publication of the CLAW hypothesis (Charlson et al., 1987),
7 extensive investigations have been undertaken into DMS formation and destruction pathways, ocean-atmosphere
8 transfer, and atmospheric transformation and impacts on chemistry and climate (Law et al., 2013; Liss and
9 Johnson, 2014; Carpenter et al., 2012; Quinn and Bates, 2011). Methanethiol or methyl mercaptan (MeSH) is
10 another reduced volatile organic sulfur gas which originates in the ocean, with a global ocean source estimated to
11 be ~17% of the DMS source. The MeSH ocean source is twice as large as the total of all anthropogenic sources
12 (Lee and Brimblecombe, 2016). However, the importance of ocean derived MeSH as a source of sulfur to the
13 atmosphere, and the impact of MeSH and its oxidation products on atmospheric chemistry and climate has been
14 little-studied.

15 DMS and MeSH in seawater (DMS_{sw} and $MeSH_{sw}$) are both produced from precursor dimethylsulfoniopropionate
16 (DMSP), which is biosynthesised by different taxa of phytoplankton and released into seawater as a result of
17 aging, grazing, or viral attack (Yoch, 2002). DMSP is then degraded by bacterial catabolism (enzyme catalysed
18 reaction) via competing pathways that produce either DMS or MeSH (Yoch, 2002). Recent research showed that
19 bacterium *Pelagibacter* can simultaneously catabolise both DMS_{sw} and $MeSH_{sw}$ (Sun et al., 2016), although it is
20 not known how widespread this phenomenon is. DMS may also be produced by phytoplankton that directly cleave
21 DMSP into DMS (Alcolombri et al., 2015). Once released, $MeSH_{sw}$ and DMS_{sw} undergo further reaction in
22 seawater. These compounds may be assimilated by bacteria, converted to dissolved non-volatile sulfur, be
23 photochemically destroyed, or in the case of $MeSH_{sw}$, react with dissolved organic matter (DOM) (Kiene and
24 Linn, 2000; Kiene et al., 2000; Flöck and Andreae, 1996). $MeSH_{sw}$ has a much higher loss rate constant than
25 DMS_{sw} , with a lifetime on the order of minutes to an hour, compared to ~days for DMS_{sw} (Kiene, 1996; Kiene
26 and Linn, 2000). A fraction (~10%) of DMS_{sw} ventilates to atmosphere where it can influence particle numbers
27 and properties through its oxidation products (Simó and Pedrós-Alió, 1999; Malin, 1997). The fraction of $MeSH_{sw}$
28 ventilating to the atmosphere is poorly constrained.

29

30 While DMS_{sw} measurements are relatively widespread, only a few studies have measured $MeSH_{sw}$. During an
31 Atlantic Meridional Transect cruise in 1998 (Kettle et al., 2001) $MeSH_{sw}$ was higher in coastal and upwelling
32 regions with the ratio of DMS_{sw} to $MeSH_{sw}$ varying from unity to 30. Leck et al (1991) also reported ratios of
33 $DMS_{sw}/MeSH_{sw}$ of 16, 20 and 6 in the Baltic, Kattegat/Skagerrak and North Seas respectively. The drivers of this
34 variability are unknown, but likely due to variation in the dominant bacterial pathway and/or spatial differences
35 in degradation processes. More recent $MeSH_{sw}$ measurements in the subarctic NE Pacific Ocean showed the ratio
36 of $DMS_{sw}/MeSH_{sw}$ varied from 2-5 indicating that $MeSH_{sw}$ was a significant contributor to the volatile sulfur pool
37 in this region (Kiene et al., 2017). $MeSH_{sw}$ measurements from these three studies (Kettle et al., 2001; Leck and
38 Rodhe, 1991; Kiene et al., 2017) were also used to calculate the ocean-atmosphere flux of MeSH, assuming control
39 from the water side. The flux of MeSH/(MeSH+DMS) ranged from 4-5% in the Baltic and Kattegat sea and 11%
40 in the North Sea (Leck and Rodhe, 1991), 16% over the North/South Atlantic transect (Kettle et al., 2001), and



1 ~15% over the North East Sub-arctic Pacific (Kiene et al., 2017). In a review of global organosulfide fluxes, Lee
2 and Brimblecombe (2016) estimated that ocean sources provide over half of the total global flux of MeSH to the
3 atmosphere, with a total 4.7 Tg S a^{-1} , however this estimate is based on a voyage-average value from a single
4 study (Kettle et al., 2001) in which flux measurements varied by several orders of magnitude.
5
6 There are very few published atmospheric measurements of MeSH_a over the ocean. To the best of our knowledge,
7 the only prior MeSH_a measurements over the ocean were made in 1986 over the Drake Passage and the coastal
8 and inshore waters west of the Antarctic Peninsula (Berresheim, 1987). MeSH_a was detected occasionally at up
9 to 3.6 ppt, which was roughly 3% of the measured atmospheric DMS_a levels (Berresheim, 1987).
10
11 Once MeSH_{sw} is transferred from ocean to atmosphere (MeSH_a), the main loss pathway for MeSH_a is via reaction
12 with OH and NO_3 radicals. MeSH_a reacts with OH at a rate 2-3 times faster than DMS, and as such MeSH_a has
13 an atmospheric lifetime of only a few hours (Lee and Brimblecombe, 2016). The oxidation pathways and products
14 that result from MeSH_a degradation are still highly uncertain (Lee and Brimblecombe, 2016; Tyndall and
15 Ravishankara, 1991), though may be somewhat similar to DMS (Lee and Brimblecombe, 2016). This leads to
16 uncertainty around the final atmospheric fate of the sulfur emitted via MeSH and also the overall impact of MeSH_a
17 oxidation on atmospheric chemistry, particularly in regions where MeSH is a significant proportion of total sulfur
18 emitted.
19 For oxygenated VOCs (OVOCs), whether the ocean acts as a source or a sink in a particular region depends on
20 the concentration gradient between seawater and atmosphere (Carpenter et al., 2012). In the case of acetone,
21 positive fluxes from the ocean have been observed in biologically productive areas (Taddei et al., 2009) and over
22 some subtropical ocean regions (Beale et al., 2013; Yang et al., 2014a; Tanimoto et al., 2014; Schlundt et al.,
23 2017), however in other subtropical regions, and generally in oligotrophic waters and at higher latitudes, net fluxes
24 are zero (e.g. ocean and atmosphere in equilibrium), or negative (transfer of acetone into ocean) (Yang et al.,
25 2014a; Marandino et al., 2005; Beale et al., 2015; Yang et al., 2014b; Schlundt et al., 2017). Atmospheric acetone
26 (acetone_a) also has significant terrestrial sources including direct biogenic emissions from vegetation, oxidation
27 of anthropogenic and biogenic hydrocarbons, (predominantly alkanes) and biomass burning (Fischer et al., 2012).
28 In the ocean, acetone_{sw} is produced photochemically from Chromophoric Dissolved Organic Matter (CDOM),
29 either directly by direct photolysis or via photosensitizer reactions (Zhou and Mopper, 1997; Dixon et al., 2013;
30 de Bruyn et al., 2012; Kieber et al., 1990). There is also evidence of direct biological production by marine bacteria
31 (Nemecek-Marshall et al., 1995) and phytoplankton (Schlundt et al., 2017; Sinha et al., 2007; Halsey et al., 2017).
32 Furthermore, acetone_{sw} has been found to decrease with depth (Beale et al., 2015; Yang et al., 2014a; Beale et al.,
33 2013; Williams et al., 2004), pointing to the importance of photochemistry and/or biological activity as the source.
34 Studies have shown acetone_{sw} production linked to photosynthetically active radiation (PAR) and net shortwave
35 radiation (Sinha et al., 2007; Beale et al., 2015; Zhou and Mopper, 1997), and Beale et al (2015) found higher
36 acetone_{sw} concentrations in spring and summer compared to autumn and winter. Removal processes include
37 uptake of acetone by bacteria as a carbon source (Beale et al., 2013; Halsey et al., 2017; Beale et al., 2015; Dixon
38 et al., 2013), gas transfer into the atmosphere, vertical mixing into the deep ocean, and photochemical destruction
39 (Carpenter and Nightingale, 2015).



1 There are relatively few observations of acetone_{sw} and acetone_a over the remote ocean, particularly in mid and
2 high latitude regions. An understanding of the spatial distribution of acetone is particularly important due to the
3 high degree of regional variation in the direction and magnitude of the acetone flux.
4
5 In this work, DMS_a, MeSH_a and acetone_a measurements were made over a biologically productive region of the
6 remote South West Pacific Ocean. The relationships between atmospheric levels of these gases are explored, as
7 well as the relationship with ocean biogeochemical parameters. The importance of MeSH as a source of sulfur to
8 the atmosphere in this region is estimated and compared to other studies. Finally, we present results from a DMS_a
9 method comparison which was undertaken at sea between three independently calibrated measurement
10 techniques.

11 **2 Method**

12 **2.1 Voyage**

13 The Surface Ocean Aerosol Production (SOAP) voyage took place on the NIWA RV *Tangaroa* over the
14 biologically productive frontal waters of Chatham Rise (44°S, 174–181°E), east of New Zealand in the South West
15 Pacific Ocean. The 23 day voyage took place during the austral summer in February – March 2012. The scientific
16 aim was to investigate interactions between the ocean and atmosphere, and as such the measurement program
17 included comprehensive characterisation of ocean biogeochemistry, measurement of ocean-atmosphere gas and
18 particle fluxes and measurement of trace gases and aerosols distribution and composition in the marine boundary
19 layer (MBL) (Law et al., 2017). During the voyage, NASA MODIS ocean colour images and underway sensors
20 were used to identify and map phytoplankton blooms. Three blooms were intensively targeted for measurement:
21 1) a dinoflagellate bloom with elevated Chl *a*, DMS_{sw} and pCO₂ drawdown and high irradiance (bloom 1-B1), 2)
22 a coccolithophore bloom (bloom 2 – B2) and 3) a mixed community bloom of coccolithophores, flagellates and
23 dinoflagellates sampled before (bloom 3a – B3a) and after (bloom 3b – B3b) a storm. For further voyage and
24 measurement details see Law et al., (2017).

25 **2.2 PTR-MS**

26 A high sensitivity proton transfer reaction mass spectrometer (PTR-MS) (Ionicon Analytik) was used to measure
27 DMS, acetone and methanethiol. The PTR-MS sampled from a 25 m 3/8 inch ID PFA inlet line which drew air
28 from the crow's nest of the vessel, 28 m above sea level (a.s.l) at 10 L min⁻¹. A baseline switch based on relative
29 wind speed and direction was employed to minimise flow of ship exhaust down the inlet (see Lawson et al., 2015).
30

31 PTR-MS instrument parameters were as follows: inlet and drift tube temperature of 60°C, a 600V drift tube and
32 2.2 mbar drift tube pressure (133 Td). The O₂ signal was <1% of the primary ion H₃O⁺ signal. DMS, acetone and
33 MeSH were measured at m/z 63, 59 and 49 respectively with a dwell time of 10s. From day of year (DOY) 43 –
34 49, 19 selected ions including m/z 59 and m/z 63 were measured resulting in 17 mass scans per hour, however
35 from DOY 49 the PTR-MS measured in scan mode from m/z 21–155, allowing three full mass scans per hour. As
36 such, MeSH measurements (m/z 49) were made only from DOY 49 onward.

37



1 VOC-free air was generated using a platinum-coated glass wool catalyst heated to 350°C; 4 times per day this air
2 was used to measure the background signal resulting from interference ions and outgassing of materials. An
3 interpolated background signal was used for background correction. Calibrations of DMS and acetone were
4 carried out daily by diluting calibration gas into VOC – free ambient air (Galbally et al. 2007). Calibration gases
5 used were a custom ~1 ppm VOC mixture in nitrogen containing DMS and acetone (Scott Specialty gases) and a
6 custom ~1 ppm VOC calibration mixture in nitrogen containing acetone (Apel Riemer). The calibration gas
7 accuracy was $\pm 5\%$. A calibration gas for MeSH was not available during this voyage. The instrument response
8 factor for DMS at m/z 63 was also applied to MeSH at m/z 49. DMS and MeSH have similar collision rate
9 constants (Williams et al., 1998) and m/z 63 and m/z 49 had the same transmission efficiency. The instrument
10 response to DMS and acetone varied by 2% and 5% throughout the voyage respectively.

11

12 In this work m/z 59 is assumed to be dominated by acetone. Propanal could also contribute to m/z 59, although
13 studies suggest this is likely low (Beale et al., 2013; Yang et al., 2014a). Similarly, m/z 49 has been attributed to
14 methanethiol, based on a literature review (Feilberg et al., 2010; Sun et al., 2016), and a lack of likely other
15 contributing species at m/z 49 in the MBL. As such m/z 59 and m/z 49 represent an upper limit for acetone and
16 MeSH respectively.

17

18 The minimum detectable limit (MDL) for a single 10s measurement of a selected mass was determined using the
19 principles of ISO 6879 (ISO, 1995). Average detection limits for the entire voyage were as follows: m/z 59
20 (acetone) 24 ppt, m/z 63 (DMS) 22 ppt, m/z 49 (MeSH) 10 ppt. The percentage of 10s observations above
21 detection limits were as follows - m/z 59 100%; m/z 63 98%; and m/z 49 63%. Inlet losses were determined to
22 be $< 2\%$ for isoprene, monoterpenes, methanol and dimethyl sulfide. Acetone and MeSH losses were not
23 determined.

24 **2.2 DMS Intercomparison**

25 During the SOAP voyage DMS_a measurements were made using three independently calibrated instruments;
26 Atmospheric Pressure Ionisation-Chemical Ionisation Mass Spectrometer (mesoCIMS) from the University of
27 California Irvine (UCI), (Bell et al., 2013, 2015), an Ionicon PTR-MS operated by CSIRO (Lawson et al., 2015),
28 and a HP Gas Chromatograph with Sulfur Chemiluminescence Detector (GC-SCD) operated by NIWA (Walker
29 et al., 2016).

30

31 Details of the mesoCIMS and GC-SCD measurement systems are provided by Bell et al. (2015) and Walker et al.
32 (2016) with a brief description provided here. The mesoCIMS instrument (Bell et al., 2013) ionizes DMS to DMS-
33 H⁺; m/z=63) by atmospheric pressure proton transfer from H₃O⁺ by passing a heated air stream over a radioactive
34 nickel foil (Ni-63). The mesoCIMS drew air from the eddy covariance set up on the bow mast at approximately
35 12m a.s.l. The inlet was a 1/2" ID PFA tube with a total inlet length of 19m and a turbulent flow at 90 SLPM.
36 The mesoCIMS sub-sampled from the inlet at 1 L m⁻¹. A gaseous tri-deuterated DMS standard (D3-DMS) was
37 added to the air sample stream at the entrance to the inlet. The internal standard was ionized and monitored
38 continuously in the mass spectrometer at m/z=66, and the atmospheric DMS mixing ratio was computed from the



1 measured 63/66 ratio. The internal standard was delivered from a high pressure aluminium cylinder and calibrated
2 against a DMS permeation tube prior to and after the cruise (Bell et al., 2015).

3

4 The GC-SCD system included a semi-automated purge and trap system, a HP 6850 gas chromatograph with
5 cryogenic preconcentrator/thermal desorber and sulfur chemiluminescence detection (Walker et al 2016). The
6 system was employed during the voyage for discrete DMS seawater measurements and gradient flux measurement
7 bag samples (Smith et al., 2018). The system was calibrated using an internal methylethylsulfide (MES)
8 permeation tube and external DMS permeation tube located in a Dynacalibrator with a twice daily 5-point
9 calibration and a running standard every 12 samples (Walker et al., 2016).

10

11 A DMS measurement intercomparison between the mesoCIMS, GC-SCD and PTR-MS was performed during the
12 voyage on DOY 64 and DOY 65. Tedlar bags (70 L) with blackout polythene covers were filled with air containing
13 DMS at sub-ppb levels and were sequentially distributed between all instruments for analysis within a few hours.
14 On DOY 64, two bags were prepared including ambient air filled from the foredeck and a DMS standard prepared
15 using a permeation device (Dynacalibrator) and dried compressed air (DMS range 384 – 420 ppt from permeation
16 uncertainty). On DOY 65, two additional bags were prepared including one ambient air from the foredeck with
17 tri-deuterated DMS added and a DMS standard prepared using the Dynacalibrator and dried compressed air (DMS
18 range 331 – 363 ppt). MesoCIMS values are not available for DOY 64 due to pressure differences between bag
19 and instrument calibration measurements; this was resolved by using an internal standard on DOY 65. For those
20 analyses, the mesoCIMS and PTR-MS measured DMS at m/z 63 and tri-deuterated DMS at m/z 66, while the
21 GC-SCD measured both DMS and deuterated DMS as a single peak.

22 **2.4 Biogeochemical measurements in surface waters**

23 Continuous seawater measurements were obtained from surface water sampled by an intake in the vessel's bow
24 at a depth of ~7m during the SOAP voyage and included underway temperature and salinity (Seabird
25 thermosalinograph SBE-21), underway chlorophyll *a* (Chl *a*) and backscatter (Wetlabs (Seabird) ECOTriplet),
26 pCO₂ (Currie et al., 2011), dissolved DMS (DMS_{sw}) (miniCIMS) (Bell et al., 2015). Quenching obscured the Chl
27 a signal during daylight when irradiance >50 W m⁻².

28

29 The following parameters were measured in surface waters (depths 2-10 m) in discrete samples from Niskin
30 bottles on a CTD rosette: nutrients according to methods described in Law et al., (2011), particulate nitrogen
31 concentration (Nodder et al., 2016), phytoplankton speciation, groups and numbers (optical microscopy of
32 samples preserved in Lugol's solution) (Safi et al., 2007), Flow cytometry, (Hall and Safi, 2001). In addition,
33 organic parameters measured included High Molecular Weight reducing sugars (Somogyi, 1926, 1952; for details
34 see Burrell (2015)) and CDOM measured using a Liquid Waveguide Capillary Cell (Gall et al., 2013). See Law
35 et al., (2017) for further details and results for these parameters.



1 **3 Results and discussion**

2 **3.1 DMS atmospheric intercomparison**

3 This section describes a comparison of DMS_a measurements from bag samples of ambient air and DMS standard
4 mixtures (analysed by GC-SCD, PTR-MS and mesoCIMS, see Section 2), as well as comparison of ambient DMS_a
5 measurements (PTR-MS and mesoCIMS).

6 **Comparison of bag samples**

7 Table 1 summarises the comparison between the GC-SCD, PTR-MS and mesoCIMS instruments for ambient and
8 DMS standard bags prepared and analysed on DOY 64 and 65 (see Section 2.2). The highest DMS levels were
9 measured by the mesoCIMS with GC-SCD and PTR-MS ~20-25 % and ~20-30% lower respectively. The GC-
10 SCD and PTR-MS agreed reasonably well, with a mean difference of 5% (range 0-10%) between instruments for
11 different diluted standard and ambient air bags. There was no clear influence of dry versus humid (ambient) bag
12 samples on the differences between instruments.

13 **Comparison of in situ ambient measurements**

14 Measurements from the PTR-MS and mesoCIMS were interpolated to a common time stamp for comparison and
15 differences examined only where data were available for both instruments. PTR-MS results for DMS were
16 reported for 10 s every 4 minutes until DOY 49 and then 10 s every 20 minutes until the end of the voyage (Section
17 2.2). The mesoCIMS measured DMS continuously and reported 10 minute averages. As such the PTR-MS
18 measured only a 'snapshot' of the DMS_a levels in each measurement cycle of 4 or 20 minutes. This was a potential
19 source of difference between the two instruments when DMS levels changed rapidly (Bell et al., 2015).

20
21 The PTR-MS and mesoCIMS drew air from separate intakes, with heights of 28 m and 12 m a.s.l, respectively.
22 As such, a further source of the difference between the PTR-MS and mesoCIMS measurements is likely due to
23 vertical gradients in DMS caused by turbulent mixing of the local surface DMS flux into the atmospheric surface
24 layer. On days with a strong DMS source and/or more stable stratification in the boundary layer, a significant
25 decrease with height is expected (Smith et al., 2018). If all the DMS observed was due to local emissions, the
26 vertical gradient would be described by Equation 2 from Smith et al (2018):

27
28
$$F \equiv -u^* * C^* = -\frac{u^* k}{\varphi c (z/L)} \left(\frac{\partial C}{\partial \ln z} \right) \quad (1)$$

29
30 Where u^* is friction velocity, C^* is scaling parameter for gas concentration, k is the von Kármán constant, φc is
31 the stability function for mass, z is the height above mean water level and L is the Monin-Obukhov scaling length
32 representing atmospheric stability.

33
34 Figure 1 shows wind speed, absolute wind direction and atmospheric stability, DMS_a levels from the voyage
35 measured by PTR-MS and mesoCIMS, relative percent difference between the two measurements (normalised to
36 the mesoCIMS), and observed absolute difference in DMS_a between the two measurements, as well as the
37 expected calculated difference (Eq 1) between two measurements due to the DMS_a concentration gradient.



1 The mesoCIMS and PTR-MS DMS_a data showed similar temporal behaviour over the voyage (Fig. 1). From DOY
2 44 – 46 there was an average of 50% ($\pm 10\%$) relative difference between measurements, yet on DOY 47 this
3 difference decreased suddenly to an average of $\sim 20\%$ ($\pm 20\%$). The reason for this change at DOY 47 is unknown.
4 Overall, agreement between instruments improved with time during the voyage, with differences of several
5 hundred ppt of DMS observed in the first few days decreasing to differences of only 10-20 ppt by the end of the
6 voyage. The agreement between instruments improves with increasing wind speeds (Fig. 1). The expected
7 calculated difference between DMS_a at the two inlet heights due to the DMS concentration gradient also decreases
8 throughout the voyage. This indicates that the increasing agreement between instruments during the voyage was
9 likely influenced by a progressively well mixed atmosphere leading to weaker DMS vertical gradients. Prior to
10 DOY 47 the difference between PTR-MS and mesoCIMS appears to have been due to instrument calibration or
11 other instrument differences rather than the DMS concentration gradient.
12
13 Figure 2a shows paired DMS_a data from the mesoCIMS versus PTR-MS over the whole voyage and Fig 2b shows
14 paired mesoCIMS data versus PTR-MS data converted to same height as the mesoCIMS with the expected DMS
15 difference calculated from the eddy covariance estimate of DMS flux (from mesoCIMS) and eddy diffusivity
16 (PTR-MS DMS_a + calculated difference between the two intake heights). The reduced major axis regression
17 relationship between the two measurements systems for uncorrected data gives a slope of 0.74 ± 0.02 , while for
18 the corrected data gives 0.81 ± 0.02 . The gradient-corrected slope agrees with the ambient bag sample ratio from
19 the method comparison (PTR-MS / mesoCIMS = 0.81 ± 0.16) (Table 1). Correcting for the DMS gradient
20 improved the comparison between PTR-MS and mesoCIMS. The remaining $\sim 20\%$ difference is likely due to
21 instrument calibration differences and differing approaches of integrated versus discrete measurements.
22
23 There was no obvious impact of absolute wind direction on the differences observed between measurement
24 systems. Note that due to the Baseline switch which was employed to avoid sampling ship exhaust down the PTR-
25 MS inlet (Lawson et al., 2015) the PTR-MS did not sample during certain relative wind directions. However, this
26 does not affect the comparison which was undertaken only when data were available for both instruments.
27
3.2 Ambient atmospheric data
28 Atmospheric mixing ratios of MeSH_a, DMS_a and acetone_a are shown along the voyage track in Fig. 3 with bloom
29 locations highlighted. Figure 4 shows a time series of MeSH_a, DMS_a, acetone_a, MeSH_a/DMS_a (all measured with
30 PTR-MS) as well as DMS_{sw} (miniCIMS) from Bell et al (2015), Chla, irradiance, wind speed, wind direction and
31 sea and air temperature. Note that MeSH_a measurements started on DOY 49, the last day of bloom B1. The fraction
32 of back trajectories arriving at the ship that had been in contact with land masses in the previous 10 days is also
33 shown with a value of 0 indicating no contact with land masses in the preceding 10 days. This was calculated
34 using the Lagrangian Numerical Atmospheric-dispersion Modelling Environment (NAME) for the lower
35 atmosphere (0–100 m) as time-integrated particle density (g s m^{-3}), every 3 hours from ship location (Jones et al,
36 2007) as shown in Law et al. (2017). Where air contacted land masses this was the New Zealand land mass in
37 almost all cases.
38



1 MeSH_a ranged from below detection limit (< 10 ppt) to 65 ppt, DMS_a ranged from below detection limit (~22 ppt)
2 up to 957 ppt, and acetone_a ranged from 50-1500 ppt (Table 2). The ratio of MeSH_a to DMS_a ranged from 0.03 -
3 0.36 for measurements when both were above the MDL. Periods of elevated DMS_a generally correspond to periods
4 of elevated DMS_{sw}. Both DMS_a and DMS_{sw} were very high during B1, during the transect to B2, and the first half
5 of B2 occupation. MeSH_a variability broadly correlates with DMS_a and DMS_{sw}, with highest levels during B2
6 (no data available for B1). The highest acetone_a levels observed occur during B2, and a broad acetone peak during
7 B1 of 700 ppt (~DOY 49) overlaps with but is slightly offset from the largest DMS_a peak during the voyage
8 (~957 ppt). DMS_a, acetone_a and MeSH_a were somewhat lower during B3a and lowest during the B3b, the post-
9 storm part of that bloom B3 (see Law et al., 2017). In general, DMS_a levels during B1 were at the upper range of
10 those found in prior studies elsewhere (Lana et al., 2011; Law et al., 2017). MeSH_a levels during B1 were
11 substantially higher than the only comparable measurements from the Drake Passage and the coastal and inshore
12 waters west of the Antarctic Peninsula (3.6 ppt) (Berresheim, 1987). The average acetone_a levels during this study
13 were broadly comparable to those from similar latitudes reported in the South Atlantic and Southern Ocean
14 (Williams et al., 2010) and at Cape Grim (Galbally et al., 2007). Acetone_a during SOAP was generally lower than
15 at similar latitudes at Mace Head (Lewis et al., 2005), the Southern Indian Ocean (Colomb et al., 2009) and also
16 the marine subtropics (Read et al., 2012; Schlundt et al., 2017; Warneke and de Gouw, 2001; Williams et al., 2004).
17
18 There were two occasions when elevated acetone_a corresponded closely to increased land influence – during B1
19 on DOY 48 - 49 (maximum land influence 12%) and DOY 60 (maximum land influence 20%) (Fig 4). Both these
20 periods corresponded to winds from the north, and back trajectories show that the land mass contacted was the
21 southern tip of New Zealand's North Island (including the city of Wellington and the northern section of the South
22 Island in both cases). The acetone measured during these periods may have been emitted from anthropogenic and
23 biogenic sources and from photochemical oxidation of hydrocarbon precursors (Fischer et al., 2012). The acetone
24 enhancement relative to the degree of land influence was higher on DOY 48 – 49 than DOY 60 possibly due to
25 different degrees of dilution of the terrestrial plume, or different terrestrial source strengths.
26 The period with the highest acetone levels during B2 (1508 ppt) corresponds with a period of negligible land
27 influence (0.3%) indicating a non-terrestrial, possibly local source of acetone_a. Neither MeSH_a or DMS_a maxima
28 corresponded with peaks in land influence, except for the latter part of the DMS_a maximum on DOY 48-49;
29 however the source of DMS_a during DOY 48 – 49 is attributed to local ocean emissions as shown by strong
30 association between DMS_{sw} and DMS_a during this period (Fig. 4).
31
32 Correlations of DMS_a, MeSH_a and acetone_a were examined to identify possible common marine sources or
33 processes influencing atmospheric levels (Table 3). Only data above MDL were included in the regressions.
34 Acetone_a data likely influenced by terrestrial sources (DOY 48-49 and 60, described above) were removed from
35 this analysis. A moderate correlation ($R^2=0.5$, $p<0.0001$) was found between DMS_a and MeSH_a during B2 with
36 a correlation of $R^2=0.3$, ($p<0.0001$) between DMS_a and MeSH_a for all data (Fig. 5). During B2 the slope was 0.13
37 (MeSH_a roughly 13% of the DMS_a mixing ratios), while for all data the slope was 0.07 (including blooms and
38 transiting between blooms).
39



1 MeSH_{sw} and DMS_{sw} are produced from bacterial catabolism of DMSP via two competing processes, so the amount
2 of DMS_{sw} vs MeSH_{sw} produced from DMSP will depend on the relative importance of these two pathways at any
3 given time. Additional sources of DMS_{sw}, such as phytoplankton that cleave DMSP into DMS will also influence
4 the amount of DMS_{sw} vs MeSH_{sw} produced. A phytoplankton-mediated source of DMS_{sw} was likely to be an
5 important contributor to the DMS_{sw} pool during the SOAP voyage, either through indirect processes (zooplankton
6 grazing, viral lysis and senescence) or direct processes (algal DMSP-lyase activity) (Lizotte et al., 2017). The
7 relative loss rates of DMS_{sw} and MeSH_{sw} through oxidation, bacterial uptake or reaction with DOM will also
8 influence the amount of each gas available to transfer to the atmosphere, with MeSH_{sw} having a much faster loss
9 rate in seawater than DMS_{sw} (Kiene and Linn, 2000; Kiene et al., 2000). Differences between the gas transfer
10 velocities of DMS and MeSH would also affect the atmospheric mixing ratios. Such differences are likely to be
11 small, due to similar solubilities (Sander, 2015) and diffusivities (Johnson, 2010) (see Section 3.4). A final factor
12 that will influence the slope of DMS_a vs MeSH_a is the atmospheric lifetime (Table 2). The average lifetimes of
13 DMS_a and MeSH_a in this study are estimated at 24 and 9 hours respectively with respect to OH, calculated using
14 DMS reaction rate of OH from Berresheim et al. (1987), the MeSH reaction rate from Atkinson et al. (1997) and
15 OH concentration calculated as described in Lawson et al. (2015). Hence, the correlation between DMS_a and
16 MeSH_a reflects the common seawater source of both gases, while the differing slopes between B2 and all data
17 probably reflect the different sources and atmospheric lifetimes. While a correlation between MeSH and DMS
18 has been observed in seawater samples previously (Kettle et al., 2001; Kiene et al., 2017), to our knowledge this
19 is the first time that a correlation between MeSH_a and DMS_a has been observed in the atmosphere over the remote
20 ocean.

21

22 There were several weak ($R^2 \leq 0.2$) but significant correlations between DMS_a and acetone_a, and acetone_a and
23 MeSH_a (Table 3). The correlation of acetone_a with DMS_a may reflect elevated organic sources for photochemical
24 production of acetone in regions of high dissolved sulfur species. A further discussion of drivers of DMS_a, acetone_a
25 and MeSH_a mixing ratios is provided in Section 3.3.

26

27 Figure 6 shows the voyage-average diurnal cycles for DMS_a, MeSH_a and acetone_a. The diurnal cycle of DMS_a
28 shows variations by almost a factor of 3 from morning (maximum at 8:00 hrs ~ 330 ppt) to late afternoon
29 (minimum, 16:00 hrs ~ 120 ppt). A DMS_a diurnal cycle with sunrise maximum and late afternoon minimum has
30 been observed in many previous studies and is attributed to photochemical destruction by OH. This includes Cape
31 Grim baseline station which samples air from the Southern Ocean (average minimum and maximum ~40-70 ppt)
32 (Ayers and Gillett, 2000), over the tropical Indian ocean (average minimum and maximum ~25-60 ppt) (Wameke
33 and de Gouw, 2001) and at Kiritimati in the tropical Pacific (average minimum and maximum 120-200 ppt) (Bandy
34 et al., 1996). The higher atmospheric levels in this study are due to high DMS_{sw} concentrations (>15 nM). The
35 amplitude of the DMS diurnal cycle is likely to have been influenced by stationing the vessel over blooms with
36 high DMS_{sw} from 8:00 hrs each day and regional mapping of areas with lower DMS_{sw} overnight (Law et al., 2017).

37

38 The diurnal cycle for MeSH_a (Fig. 6 b) shows similar behaviour to DMS_a with the mixing ratios varying by a
39 factor of ~2 with the minimum mixing ratio occurring at around 16:00 hrs (the same time as minimum DMS_a).



1 The most important sink of MeSH_a is thought to be oxidation by OH (Lee and Brimblecombe, 2016), and the
2 minima in late afternoon may be due to destruction by OH.
3
4 The acetone_a diurnal cycle (Fig. 6c) with land-influenced data removed shows reasonably consistent mixing ratios
5 from the early morning until midday, with an overall increase in acetone levels during the afternoon hours from
6 14:00 hrs onwards, then decreasing again at night, which is the opposite to the behaviour of DMS_a and MeSH_a .
7 Acetone is long lived (~60 days – Table 2) with respect to oxidation by OH. The increase of acetone_a mixing
8 ratios in the afternoon may indicate photochemical production from atmosphere or sea surface precursors but there
9 was no correlation between irradiance and acetone_a during the voyage.

10 **3.3 Flux calculation from nocturnal accumulation of MeSH**

11 MeSH and DMS fluxes (F) were calculated according to the nocturnal accumulation method (Marandino et al.,
12 2007). This approach assumes that nighttime photochemical losses are negligible, and that sea surface emissions
13 accumulate overnight within the well-mixed marine boundary layer (MBL). Horizontal homogeneity and zero
14 flux at the top of the boundary layer are also assumed. The air-sea flux is calculated from the increase in MeSH
15 and DMS. For example:

16

17
$$F = \frac{\partial [\text{MeSH}]}{\partial t} \times h \quad (2)$$

18

19 where $[\text{MeSH}]$ is the concentration of MeSH in mol m^{-3} and h = average nocturnal MBL for the voyage of 1135
20 $\text{m} \pm 657 \text{ m}$, estimated from nightly radiosonde flights.

21 DMS and MeSH fluxes were calculated for 3 nights (DOY 52, 54 and 60) (Table 4) when linear increases in
22 mixing ratios occurred over several hours (Fig 4). The MeSH flux was lowest on DOY 52 prior to B2 (3.5 ± 2
23 $\mu\text{mol}^{-1} \text{ m}^2 \text{ day}^{-1}$), higher on DOY 60 during B3a ($4.8 \pm 2.8 \mu\text{mol}^{-1} \text{ m}^2 \text{ day}^{-1}$), and highest on DOY 42 during B2
24 ($5.8 \pm 3.4 \mu\text{mol}^{-1} \text{ m}^2 \text{ day}^{-1}$). There are no MeSH measurements during B1. The percentage of
25 MeSH/(DMS+MeSH) emitted varied from 14% for DOY 60 (B3a), up to 23% and 24% for DOY 54 (B2) and
26 DOY 52 (prior to B2).

27 For comparison the DMS fluxes measured using eddy covariance (EC) at the same time are given in Table 4 (Bell
28 et al., 2015). DMS fluxes calculated using the nocturnal accumulation method are within the variability of the EC
29 fluxes (Bell et al., 2015).

30 The average MeSH flux calculated from this study ($4.7 \mu\text{mol m}^{-2} \text{ day}^{-1}$) was more than 4 times higher than average
31 MeSH fluxes from previous studies in the North/South Atlantic (Kettle et al., 2001) and in the Baltic, Kattegat
32 and North Sea (Leck and Rodhe, 1991) (Table 5). The MeSH fluxes calculated from this work are comparable to
33 maximum values reported by Kettle et al., (2001) which were observed in localised coastal and upwelling regions.
34 The average emission of MeSH compared to DMS (MeSH/(DMS+MeSH)) was higher in this study (20%) than
35 previous studies (Table 5) including the Baltic, Kattegat and North Sea (5%, 4% and 11%), North/South Atlantic
36 (16%), and a recent study from the Northeast Sub-arctic Pacific (~15%) (Kiene et al., 2017). Note that other
37 sulfur species such as dimethyl disulphide (DMDS), carbon disulphide (CS_2) and hydrogen sulphide (H_2S)
38 typically make a very small contribution to the total sulfur compared to DMS and MeSH (Leck and Rodhe,
39 1991; Kettle et al., 2001; Yvon et al., 1993) and so are neglected from this calculation.



1 **3.4 Correlation with ocean biogeochemistry**

2 To investigate the influence of biogeochemical parameters on atmospheric mixing ratios of MeSH_a , DMS_a and
3 acetone $_a$, Spearman rank correlations were undertaken to identify relationships significant at the 95% confidence
4 interval (CI). Table 6 summarises the correlation coefficients and p values for significant correlations. MeSH_a ,
5 DMS_a and acetone $_a$ data were averaged one hour either side of the CTD water entry time for the analysis.

6

7 Sulfur gases MeSH_a and DMS_a are short lived and so the air-sea flux is controlled by the seawater concentration.
8 By contrast, acetone $_a$ is much longer lived in the atmosphere (~60 days), so the air/sea gradient can be influenced
9 by both oceanic emissions and atmospheric transport from other sources. As such, the variability in acetone $_a$
10 mixing ratios may be driven by ocean/air exchange and/or input of acetone $_a$ to the boundary layer from terrestrial
11 sources, the upper atmosphere, or in situ production. This means that correlation analyses to explore ocean
12 biogeochemical sources of acetone $_a$ may be confounded by atmospheric sources. Removal of land influenced
13 data reduces the likelihood of this but observed increases in atmospheric acetone could still be from in situ
14 processes such as oxidation of organic aerosol or mixing from above the boundary layer.

15

16 Both MeSH_a and DMS_a have a strong positive and highly significant relationship with DMS_{sw} , and a moderate
17 correlation with discrete measurements of DMSP_t and DMSP_p . The correlation of DMS_a with DMS_{sw} is clear,
18 however the correlation of MeSH_a with DMS_{sw} is likely due to a common ocean precursor of both gases (DMSP)
19 albeit via different production pathways. DMS_a and MeSH_a correlate with DMSP_p (particulate) but not with
20 DMSP_d (dissolved). For DMS_a , the correlation may reflect that a proportion of the DMS observed was derived
21 directly from phytoplankton rather than being bacterially mediated, in agreement with findings by Lizotte et al.,
22 (2017); however, as demethylation of DMSP_d represents the primary source of MeSH the lack of correlation is
23 surprising. The latter may reflect MeSH sinks in surface water associated with organics and particles (Kiene,
24 1996). DMS_a also correlated with particulate nitrogen and showed a moderate negative correlation with silicate
25 that may reflect lower DMS production in diatom-dominated waters.

26

27 Acetone $_a$ shows a positive correlation with temperature and negative correlation with nutrients. This is consistent
28 with reported sources of acetone $_{\text{sw}}$ in warmer subtropical waters (Beale et al., 2013; Yang et al., 2014a; Tanimoto
29 et al., 2014; Schlundt et al., 2017). The positive relationship with organic material including HMW sugars and
30 CDOM may reflect a photochemical ocean source (Zhou and Mopper, 1997; Dixon et al., 2013; de Bruyn et al.,
31 2012; Kieber et al., 1990), or possibly a biological source (Nemecek-Marshall et al., 1995; Nemecek-Marshall et
32 al., 1999; Schlundt et al., 2017; Sinha et al., 2007; Halsey et al., 2017) as indicated by the correlations with
33 cryptophyte and picoplankton abundance. Correlation with particle backscatter suggests potential links between
34 acetone $_a$ and coccolithophores (Sinha et al., 2007). Alternatively, the positive correlations of acetone $_a$ with these
35 organic components of sea water may reflect acetone production in the atmosphere from photochemical oxidation
36 of ocean-derived organic aerosols (Pan et al., 2009; Kwan et al., 2006; Jacob et al., 2002).



1 **4 Implications and conclusions**

2 Mixing ratios of short-lived MeSH_a over the remote ocean of up to 65 ppt in this study provide evidence that
3 MeSH transfers from the ocean into the atmosphere and may be present at non-negligible levels in the atmosphere
4 over other regions of high biological productivity. The average MeSH flux calculated from this study ($4.7 \mu\text{mol}$
5 $\text{m}^{-2} \text{ day}^{-1}$) was at least 4 times higher than average MeSH fluxes from previous studies and is comparable to
6 maximum MeSH flux values reported in localised coastal and upwelling regions of the North/South Atlantic
7 (Kettle et al., 2001) (Table 5). The average emission of MeSH compared to DMS ($\text{MeSH}/(\text{DMS}+\text{MeSH})$) was
8 higher in this study (20%) than previous studies (4–16%), indicating MeSH provides a significant transfer of sulfur
9 to the atmosphere in this region. Taken together with other studies, the magnitude of the ocean MeSH flux to the
10 atmosphere appears to be highly variable as is the proportion of S emitted as MeSH compared to DMS . For
11 example, MeSH fluxes in the Kettle et al. (2001) study varied by orders of magnitude, and in some cases the
12 MeSH flux equalled the DMS flux. Similarly, studies that reported MeSH_{sw} and DMS_{sw} concentrations have
13 shown the $\text{DMS}_{\text{sw}}/\text{MeSH}_{\text{sw}}$ concentration ratios varied substantially, from 30 to unity (Kettle et al. 2001), from 6–
14 20 (Leck and Rodhe, 1991) and 2–5 (Kiene et al., 2017). As such, further studies are needed to investigate the
15 spatial distribution of MeSH both in seawater and the atmosphere as well as the importance of MeSH as a source
16 of atmospheric sulfur. The fate of atmospheric MeSH sulfur in the atmosphere is also highly uncertain, in terms
17 of its degradation pathways and reactions, and intermediate and final degradation products. For example, the
18 impact that oxidation of MeSH_a has on the oxidative capacity of the MBL and on other processes such as particle
19 formation or growth to the best of our knowledge remains largely unknown, and further work is needed on its
20 atmospheric processes and fate.

21
22 This work suggests a source of acetone from warmer subtropical ocean waters, in line with other studies, with
23 positive correlations between acetone_a and ocean temperature, high molecular weight sugars, cryptophyte and
24 eukaryote phytoplankton, chromophoric dissolved organic matter (CDOM) and particle backscatter, and a
25 negative correlation with nutrients. While data with a terrestrial source influence was removed from this analysis,
26 it is still possible that the acetone peaks observed may not have been due to a positive flux of acetone from the
27 ocean, but rather from in situ processes leading to acetone production such as oxidation of marine-derived organic
28 aerosol.

29 Finally, the SOAP voyage provided the opportunity to compare 3 independently calibrated DMS measurement
30 techniques at sea (PTR-MS, mesoCIMS and GC-SCD). Agreement was generally good, with a mean difference
31 of 5% between the PTR-MS and GC-SCD DMS diluted standard and air sample measurements, with the
32 mesoCIMS mixing ratios approximately 20–30% higher. A comparison of ambient DMS_a data during the voyage
33 for the PTR-MS and mesoCIMS showed very similar temporal behaviour, and an average difference of ~25%.
34 Correcting for the expected difference in DMS_a due to the DMS concentration gradient at the different inlet heights
35 (28 and 12 m a.s.l for the PTR-MS and mesoCIMS respectively) reduced this difference to ~20%. As such, this
36 remaining difference is likely due to instrument calibration differences and differing approaches of integrated
37 versus discrete measurements.

38

39

40



1 **Data availability**

2 DMS, acetone and MeSH data are available via the CSIRO data access portal (DAP) at
3 <https://doi.org/10.25919/5d914b00c5759>. Further data are available by emailing the corresponding author or the
4 voyage leader: cliff.law@niwa.co.nz.

5 **Author Acknowledgements**

6 We thank the officers and crew of the RV Tangaroa and NIWA Vessels for logistics support. Many thanks to John
7 McGregor (NIWA) for providing land influence data and to Paul Selleck and Erin Dunne (CSIRO) for helpful
8 discussions. Thanks to the NIWA Visiting Scientist Scheme and CSIRO's Capability Development Fund for
9 providing financial support for Sarah Lawson's participation in the SOAP voyage.

10 **References**

11
12 Alcolombri, U., Ben-Dor, S., Feldmesser, E., Levin, Y., Tawfik, D. S., and Vardi, A.: Identification of the algal
13 dimethyl sulfide-releasing enzyme: A missing link in the marine sulfur cycle, *J. Science*, 348, 1466-1469,
14 10.1126/science.aab1586, 2015.
15 Atkinson, R.: Kinetics and mechanisms of the gas-phase reactions of the hydroxyl radical with organic compounds
16 under atmospheric conditions, *Chem. Rev.*, 86, 69-201, 10.1021/cr00071a004, 1986.
17 Atkinson, R., Baulch, D. L., Cox, R. A., Jr., R. F. H., Kerr, J. A., Rossi, M. J., and Troe, J.: Evaluated Kinetic,
18 Photochemical and Heterogeneous Data for Atmospheric Chemistry: Supplement V. IUPAC Subcommittee on
19 Gas Kinetic Data Evaluation for Atmospheric Chemistry, 26, 521-1011, 10.1063/1.556011, 1997.
20 Ayers, G. P., and Gillett, R. W.: DMS and its oxidation products in the remote marine atmosphere: implications
21 for climate and atmospheric chemistry, *Journal of Sea Research*, 43, 275-286, 2000.
22 Bandy, A. R., Thornton, D. C., Blomquist, B. W., Chen, S., Wade, T. P., Ianni, J. C., Mitchell, G. M., and Nadler,
23 W.: Chemistry of dimethyl sulfide in the equatorial Pacific atmosphere, *Geophysical Research Letters*, 23, 741-
24 744, 10.1029/96gl00779, 1996.
25 Beale, R., Dixon, J. L., Arnold, S. R., Liss, P. S., and Nightingale, P. D.: Methanol, acetaldehyde, and acetone in
26 the surface waters of the Atlantic Ocean, *Journal of Geophysical Research: Oceans*, 118, 5412-5425,
27 10.1002/jgrc.20322, 2013.
28 Beale, R., Dixon, J. L., Smyth, T. J., and Nightingale, P. D.: Annual study of oxygenated volatile organic
29 compounds in UK shelf waters, *Marine Chemistry*, 171, 96-106, <https://doi.org/10.1016/j.marchem.2015.02.013>,
30 2015.
31 Bell, T. G., De Bruyn, W., Miller, S. D., Ward, B., Christensen, K. H., and Saltzman, E. S.: Air-sea
32 dimethylsulfide (DMS) gas transfer in the North Atlantic: evidence for limited interfacial gas exchange at high
33 wind speed, *Atmos. Chem. Phys.*, 13, 11073-11087, 10.5194/acp-13-11073-2013, 2013.
34 Bell, T. G., De Bruyn, W., Marandino, C. A., Miller, S. D., Law, C. S., Smith, M. J., and Saltzman, E. S.:
35 Dimethylsulfide gas transfer coefficients from algal blooms in the Southern Ocean, *Atmos. Chem. Phys.*, 15,
36 1783-1794, 10.5194/acp-15-1783-2015, 2015.
37 Berresheim, H.: Biogenic sulfur emissions from the Subantarctic and Antarctic Oceans, *Journal of Geophysical
38 Research*, 92, 13245-13262, 10.1029/JD092iD11p13245, 1987.
39 Burrell, T. J.: Bacterial extracellular enzyme activity in a future ocean, PhD, Victoria University of Wellington,
40 324 pp., 2015.
41 Carpenter, L. J., Archer, S. D., and Beale, R.: Ocean-atmosphere trace gas exchange, *Chem. Soc. Rev.*, 41, 6473-
42 6506, 10.1039/c2cs35121h, 2012.
43 Carpenter, L. J., and Nightingale, P. D.: Chemistry and Release of Gases from the Surface Ocean, *Chem. Rev.*,
44 10.1021/cr5007123, 2015.
45 Charlson, R., Lovelock, J., Andreae, M., and Warren, S.: Oceanic phytoplankton, atmospheric sulphur, cloud
46 albedo and climate., *Nature*, 326, 10.1038/326655a0, 1987.
47 Colomb, A., Gros, V., Alvain, S., Sarda-Esteve, R., Bonsang, B., Moulin, C., Klupfel, T., and Williams, J.:
48 Variation of atmospheric volatile organic compounds over the Southern Indian Ocean (30-49 degrees S),
49 *Environmental Chemistry*, 6, 70-82, 10.1071/en08072, 2009.



1 Currie, K. I., Macaskill, B., Reid, M. R., and Law, C. S.: Processes governing the carbon chemistry during the
2 SAGE experiment, *Deep Sea Research Part II: Topical Studies in Oceanography*, 58, 851-860, 2011.

3 de Bruyn, W. J., Clark, C. D., Pagel, L., and Takehara, C.: Photochemical production of formaldehyde,
4 acetaldehyde and acetone from chromophoric dissolved organic matter in coastal waters, *Journal of
5 Photochemistry and Photobiology a-Chemistry*, 226, 16-22, 10.1016/j.jphotochem.2011.10.002, 2012.

6 Dixon, J. L., Beale, R., and Nightingale, P. D.: Production of methanol, acetaldehyde, and acetone in the Atlantic
7 Ocean, *Geophysical Research Letters*, 40, 4700-4705, 10.1002/grl.50922, 2013.

8 Feilberg, A., Liu, D., Adamsen, A. P. S., Hansen, M. J., and Jonassen, K. E. N.: Odorant Emissions from Intensive
9 Pig Production Measured by Online Proton-Transfer-Reaction Mass Spectrometry, *Environmental Science &
10 Technology*, 44, 5894-5900, 10.1021/es100483s, 2010.

11 Fischer, E. V., Jacob, D. J., Millet, D. B., Yantosca, R. M., and Mao, J.: The role of the ocean in the global
12 atmospheric budget of acetone, *Geophysical Research Letters*, 39, 5, L01807
13 10.1029/2011gl050086, 2012.

14 Flöck, O. R., and Andreae, M. O.: Photochemical and non-photochemical formation and destruction of carbonyl
15 sulfide and methyl mercaptan in ocean waters, *Marine Chemistry*, 54, 11-26, [https://doi.org/10.1016/0304-4203\(96\)00027-8](https://doi.org/10.1016/0304-4203(96)00027-8), 1996.

16 Galbally, I. E., Lawson, S. J., Weeks, I. A., Bentley, S. T., Gillett, R. W., Meyer, M., and Goldstein, A. H.: Volatile
17 organic compounds in marine air at Cape Grim, Australia, *Environmental Chemistry*, 4, 178-182,
18 10.1071/en07024, 2007.

19 Gall, M. P., Davies-Colley, R. J., and Merrilees, R. A.: Exceptional visual clarity and optical purity in a sub-alpine
20 lake, *Limnology and Oceanography*, 58, 443-451, 10.4319/lo.2013.58.2.0443, 2013.

21 Hall, J. A., and Safi, K.: The impact of in situ Fe fertilisation on the microbial food web in the Southern Ocean,
22 *Deep Sea Research Part II: Topical Studies in Oceanography*, 48, 2591-2613, [https://doi.org/10.1016/S0967-0645\(01\)00010-8](https://doi.org/10.1016/S0967-0645(01)00010-8), 2001.

23 Halsey, K. H., Giovannoni, S. J., Graus, M., Zhao, Y., Landry, Z., Thrash, J. C., Vergin, K. L., and de Gouw, J.:
24 Biological cycling of volatile organic carbon by phytoplankton and bacterioplankton, *Limnology and
25 Oceanography*, 62, 2650-2661, 10.1002/lno.10596, 2017.

26 ISO: ISO 6879: Air Quality, Performance Characteristics and Related Concepts for Air Quality Measuring
27 Methods, International Organisation for Standardisation, Geneva, Switzerland, 1995.

28 Jacob, D. J., Field, B. D., Jin, E. M., Bey, I., Li, Q. B., Logan, J. A., Yantosca, R. M., and Singh, H. B.:
29 Atmospheric budget of acetone, *Journal of Geophysical Research-Atmospheres*, 107, 17, 4100
30 10.1029/2001jd000694, 2002.

31 Johnson, M. T.: A numerical scheme to calculate temperature and salinity dependent air-water transfer velocities
32 for any gas, *Ocean Sci.*, 6, 913-932, 10.5194/os-6-913-2010, 2010.

33 Jones, A. R., Thomson, D. J., Hort, M., and Devenish, B.: The UK Met Office's next-generation atmospheric
34 dispersion model, NAMEIII, in: *Proceedings of the 27th NATO/CCMS International Technical Meeting on Air
35 Pollution Modelling and its Application*, edited by: Borrego, C., and Norman, A.-L., Springer, 580-589, 2007.

36 Kettle, A. J., Rhee, T. S., von Hobe, M., Poulton, A., Aiken, J., and Andreae, M. O.: Assessing the flux of different
37 volatile sulfur gases from the ocean to the atmosphere, *Journal of Geophysical Research*, 106, 12193-12209,
38 10.1029/2000jd900630, 2001.

39 Kieber, R. J., Zhou, X., and Mopper, K.: Formation of carbonyl compounds from UV-induced photodegradation
40 of humic substances in natural waters: Fate of riverine carbon in the sea, *Limnology and Oceanography*, 35, 1503-
41 1515, 10.4319/lo.1990.35.7.1503, 1990.

42 Kiene, R. P.: Production of methanethiol from dimethylsulfoniopropionate in marine surface waters, *Marine
43 Chemistry*, 54, 69-83, [https://doi.org/10.1016/0304-4203\(96\)00006-0](https://doi.org/10.1016/0304-4203(96)00006-0), 1996.

44 Kiene, R. P., and Linn, L. J.: The fate of dissolved dimethylsulfoniopropionate (DMSP) in seawater: tracer studies
45 using ³⁵S-DMSP, *Geochimica et Cosmochimica Acta*, 64, 2797-2810, [https://doi.org/10.1016/S0016-7037\(00\)00399-9](https://doi.org/10.1016/S0016-7037(00)00399-9), 2000.

46 Kiene, R. P., Linn, L. J., and Bruton, J. A.: New and important roles for DMSP in marine microbial communities,
47 *Journal of Sea Research*, 43, 209-224, [https://doi.org/10.1016/S1385-1101\(00\)00023-X](https://doi.org/10.1016/S1385-1101(00)00023-X), 2000.

48 Kiene, R. P., Williams, T. E., Esson, K., Tortell, P. D., and Dacey, J. W. H.: Methanethiol Concentrations and
49 Sea-Air Fluxes in the Subarctic NE Pacific Ocean, *American Geophysical Union*, Fall meeting, 2017,

50 Kwan, A. J., Crounse, J. D., Clarke, A. D., Shinozuka, Y., Anderson, B. E., Crawford, J. H., Avery, M. A.,
51 McNaughton, C. S., Brune, W. H., Singh, H. B., and Wennberg, P. O.: On the flux of oxygenated volatile organic
52 compounds from organic aerosol oxidation, *Geophysical Research Letters*, 33, 10.1029/2006gl026144, 2006.

53 Lana, A., Bell, T. G., Simó, R., Vallina, S. M., Ballabriga-Poy, J., Kettle, A. J., Dachs, J., Bopp, L., Saltzman, E.
54 S., Stefels, J., Johnson, J. E., and Liss, P. S.: An updated climatology of surface dimethylsulfide concentrations
55 and emission fluxes in the global ocean, *Global Biogeochemical Cycles*, 25, 10.1029/2010gb003850, 2011.

56 Law, C. S., Brévière, E., de Leeuw, G., Garçon, V., Guieu, C., Kieber, D. J., Konradowitz, S., Paulmier, A.,
57 Quinn, P. K., Saltzman, E. S., Stefels, J., and von Glasow, R.: Evolving research directions in Surface Ocean-

58

59

60



1 Lower Atmosphere (SOLAS) science, *Environmental Chemistry*, 10, 1-16, <https://doi.org/10.1071/EN12159>,
2 2013.

3 Law, C. S., Smith, M. J., Harvey, M. J., Bell, T. G., Cravigan, L. T., Elliott, F. C., Lawson, S. J., Lizotte, M.,
4 Marriner, A., McGregor, J., Ristovski, Z., Safi, K. A., Saltzman, E. S., Vaattovaara, P., and Walker, C. F.:
5 Overview and preliminary results of the Surface Ocean Aerosol Production (SOAP) campaign, *Atmos. Chem.
6 Phys.*, 17, 13645-13667, 10.5194/acp-17-13645-2017, 2017.

7 Law, C. S., Woodward, E. M. S., Ellwood, M. J., Marriner, A., Bury, S. J., and Safi, K. A.: Response of surface
8 nutrient inventories and nitrogen fixation to a tropical cyclone in the southwest Pacific, *Limnology and
9 Oceanography*, 56, 1372-1385, 10.4319/lo.2011.56.4.1372, 2011.

10 Lawson, S. J., Selleck, P. W., Galbally, I. E., Keywood, M. D., Harvey, M. J., Lerot, C., Helmig, D., and Ristovski,
11 Z.: Seasonal in situ observations of glyoxal and methylglyoxal over the temperate oceans of the Southern
12 Hemisphere, *Atmos. Chem. Phys.*, 15, 223-240, 10.5194/acp-15-223-2015, 2015.

13 Leck, C., and Rodhe, H. J. J. o. A. C.: Emissions of marine biogenic sulfur to the atmosphere of northern Europe,
14 *Journal of Atmospheric Chemistry*, 12, 63-86, 10.1007/bf00053934, 1991.

15 Lee, C. L., and Brimblecombe, P.: Anthropogenic contributions to global carbonyl sulfide, carbon disulfide and
16 organosulfides fluxes, *Earth-Sci. Rev.*, 160, 1-18, <https://doi.org/10.1016/j.earscirev.2016.06.005>, 2016.

17 Lewis, A. C., Hopkins, J. R., Carpenter, L. J., Stanton, J., Read, K. A., and Pilling, M. J.: Sources and sinks of
18 acetone, methanol, and acetaldehyde in North Atlantic marine air, *Atmos. Chem. Phys.*, 5, 1963-1974,
19 10.5194/acp-5-1963-2005, 2005.

20 Liss, P. S., and Johnson, M. T.: *Ocean-Atmosphere Interactions of Gases and Particles*, edited by: Liss, P. S., and
21 Johnson, M. T., Springer Earth System Sciences, 315 pp., 2014.

22 Lizotte, M., Levasseur, M., Law, C. S., Walker, C. F., Safi, K. A., Marriner, A., and Kiene, R. P.:
23 Dimethylsulfoniopropionate (DMSP) and dimethyl sulfide (DMS) cycling across contrasting biological hotspots
24 of the New Zealand subtropical front, *Ocean Sci.*, 13, 961-982, 10.5194/os-13-961-2017, 2017.

25 Malin, G.: Sulphur, climate and the microbial maze, *Nature*, 387, 857-858, 10.1038/43075, 1997.

26 Marandino, C. A., De Bruyn, W. J., Miller, S. D., Prather, M. J., and Saltzman, E. S.: Oceanic uptake and the
27 global atmospheric acetone budget, *Geophysical Research Letters*, 32, 10.1029/2005gl023285, 2005.

28 Marandino, C. A., De Bruyn, W. J., Miller, S. D., and Saltzman, E. S.: Eddy correlation measurements of the
29 air/sea flux of dimethyl sulfide over the North Pacific Ocean, *Journal of Geophysical Research: Atmospheres*, 112,
30 10.1029/2006jd007293, 2007.

31 Nemecek-Marshall, M., Wojciechowski, C., Kuzma, J., Silver, G. M., and Fall, R.: Marine Vibrio species produce
32 the volatile organic compound acetone, *Appl Environ Microbiol*, 61, 44-47, 1995.

33 Nemecek-Marshall, M., Wojciechowski, C., Wagner, W. P., and Fall, R.: Acetone formation in the Vibrio family:
34 a new pathway for bacterial leucine catabolism, *J Bacteriol*, 181, 7493-7499, 1999.

35 Nodder, S. D., Chiswell, S. M., and Northcote, L. C.: Annual cycles of deep-ocean biogeochemical export fluxes
36 in subtropical and subantarctic waters, southwest Pacific Ocean, *Journal of Geophysical Research: Oceans*, 121,
37 2405-2424, 10.1002/2015jc011243, 2016.

38 Pan, X., Underwood, J. S., Xing, J. H., Mang, S. A., and Nizkorodov, S. A.: Photodegradation of secondary
39 organic aerosol generated from limonene oxidation by ozone studied with chemical ionization mass spectrometry,
40 *Atmos. Chem. Phys.*, 9, 3851-3865, 10.5194/acp-9-3851-2009, 2009.

41 Quinn, P. K., and Bates, T. S.: The case against climate regulation via oceanic phytoplankton sulphur emissions,
42 *Nature*, 480, 51-56, 10.1038/nature10580, 2011.

43 Read, K. A., Carpenter, L. J., Arnold, S. R., Beale, R., Nightingale, P. D., Hopkins, J. R., Lewis, A. C., Lee, J. D.,
44 Mendes, L., and Pickering, S. J.: Multiannual Observations of Acetone, Methanol, and Acetaldehyde in Remote
45 Tropical Atlantic Air: Implications for Atmospheric OVOC Budgets and Oxidative Capacity, *Environmental
46 Science & Technology*, 46, 11028-11039, 10.1021/es302082p, 2012.

47 Safi, K. A., Brian Griffiths, F., and Hall, J. A.: Microzooplankton composition, biomass and grazing rates along
48 the WOCE SR3 line between Tasmania and Antarctica, *Deep Sea Research Part I: Oceanographic Research
49 Papers*, 54, 1025-1041, <https://doi.org/10.1016/j.dsr.2007.05.003>, 2007.

50 Sander, R.: Compilation of Henry's law constants (version 4.0) for water as solvent, *Atmos. Chem. Phys.*, 15,
51 4399-4981, 10.5194/acp-15-4399-2015, 2015.

52 Schlundt, C., Tegtmeier, S., Lennartz, S. T., Bracher, A., Cheah, W., Krüger, K., Quack, B., and Marandino, C.
53 A.: Oxygenated volatile organic carbon in the western Pacific convective center: ocean cycling, air-sea gas
54 exchange and atmospheric transport, *Atmos. Chem. Phys.*, 17, 10837-10854, 10.5194/acp-17-10837-2017, 2017.

55 Simó, R., and Pedrós-Alió, C.: Short-term variability in the open ocean cycle of dimethylsulfide, *Glocal
56 Biogeochemical Cycles*, 13, 1173-1181, 10.1029/1999gb900081, 1999.

57 Sinha, V., Williams, J., Meyerhofer, M., Riebesell, U., Paulino, A. I., and Larsen, A.: Air-sea fluxes of methanol,
58 acetone, acetaldehyde, isoprene and DMS from a Norwegian fjord following a phytoplankton bloom in a
59 mesocosm experiment, *Atmospheric Chemistry and Physics*, 7, 739-755, 2007.



1 Smith, M. J., Walker, C. F., Bell, T. G., Harvey, M. J., Saltzman, E. S., and Law, C. S.: Gradient flux
2 measurements of sea-air DMS transfer during the Surface Ocean Aerosol Production (SOAP) experiment, *Atmos.*
3 *Chem. Phys.*, 18, 5861-5877, 10.5194/acp-18-5861-2018, 2018.

4 Somogyi, M.: Notes on Sugar Determination, *Journal of Biological Chemistry*, 70, 599-612, 1926.

5 Somogyi, M.: Notes on Sugar Determination, *Journal of Biological Chemistry*, 195, 19-23, 1952.

6 Sun, J., Todd, J. D., Thrash, J. C., Qian, Y., Qian, M. C., Temperton, B., Guo, J., Fowler, E. K., Aldrich, J. T.,
7 Nicora, C. D., Lipton, M. S., Smith, R. D., De Leenheer, P., Payne, S. H., Johnston, A. W. B., Davie-Martin, C.
8 L., Halsey, K. H., and Giovannoni, S. J.: The abundant marine bacterium *Pelagibacter* simultaneously catabolizes
9 dimethylsulfoniopropionate to the gases dimethyl sulfide and methanethiol, *Nature Microbiology*, 1, 16065,
10 10.1038/nmicrobiol.2016.65
11 <https://www.nature.com/articles/nmicrobiol201665#supplementary-information>, 2016.

12 Taddei, S., Toscano, P., Gioli, B., Matese, A., Miglietta, F., Vaccari, F. P., Zaldei, A., Custer, T., and Williams,
13 J.: Carbon Dioxide and Acetone Air-Sea Fluxes over the Southern Atlantic, *Environmental Science &*
14 *Technology*, 43, 5218-5222, 10.1021/es8032617, 2009.

15 Tanimoto, H., Kameyama, S., Iwata, T., Inomata, S., and Omori, Y.: Measurement of Air-Sea Exchange of
16 Dimethyl Sulfide and Acetone by PTR-MS Coupled with Gradient Flux Technique, *Environmental Science &*
17 *Technology*, 48, 526-533, 10.1021/es4032562, 2014.

18 Tyndall, G. S., and Ravishankara, A. R.: Atmospheric oxidation of reduced sulfur species, *International Journal*
19 *of Chemical Kinetics*, 23, 483-527, 10.1002/kin.550230604, 1991.

20 Walker, C. F., Harvey, M. J., Smith, M. J., Bell, T. G., Saltzman, E. S., Marriner, A. S., McGregor, J. A., and
21 Law, C. S.: Assessing the potential for dimethylsulfide enrichment at the sea surface and its influence on air-sea
22 flux, *Ocean Sci.*, 12, 1033-1048, 10.5194/os-12-1033-2016, 2016.

23 Wameke, C., and de Gouw, J. A.: Organic trace gas composition of the marine boundary layer over the northwest
24 Indian Ocean in April 2000, *Atmospheric Environment*, 35, 5923-5933, 2001.

25 Williams, T. L., Adams, N. G., and Babcock, L. M.: Selected ion flow tube studies of $\text{H}_3\text{O}^+(\text{H}_2\text{O})_{0,1}$ reactions with
26 sulfides and thiols, *International Journal of Mass Spectrometry and Ion Processes*, 172, 149-159,
27 [https://doi.org/10.1016/S0168-1176\(97\)00081-5](https://doi.org/10.1016/S0168-1176(97)00081-5), 1998.

28 Williams, J., Holzinger, R., Gros, V., Xu, X., Atlas, E., and Wallace, D. W. R.: Measurements of organic species
29 in air and seawater from the tropical Atlantic, *Geophysical Research Letters*, 31, 5, L23s06
30 10.1029/2004gl020012, 2004.

31 Williams, J., Custer, T., Riede, H., Sander, R., Jäckel, P., Hoor, P., Pozzer, A., Wong-Zehnpfennig, S., Hosaynali
32 Beygi, Z., Fischer, H., Gros, V., Colomb, A., Bonsang, B., Yassaa, N., Peeken, I., Atlas, E. L., Waluda, C. M.,
33 van Aardenne, J. A., and Lelieveld, J.: Assessing the effect of marine isoprene and ship emissions on ozone, using
34 modelling and measurements from the South Atlantic Ocean, *Environmental Chemistry*, 7, 171-182,
35 doi:10.1071/EN09154, 2010.

36 Yang, M., Beale, R., Liss, P., Johnson, M., Blomquist, B., and Nightingale, P.: Air-sea fluxes of oxygenated
37 volatile organic compounds across the Atlantic Ocean, *Atmos. Chem. Phys.*, 14, 7499-7517, 10.5194/acp-14-
38 7499-2014, 2014a.

39 Yang, M., Blomquist, B. W., and Nightingale, P. D.: Air-sea exchange of methanol and acetone during HiWinGS:
40 Estimation of air phase, water phase gas transfer velocities, 119, 7308-7323, 10.1002/2014jc010227, 2014b.

41 Yoch, D. C.: Dimethylsulfoniopropionate: Its Sources, Role in the Marine Food Web, and Biological Degradation
42 to Dimethylsulfide, 68, 5804-5815, 10.1128/AEM.68.12.5804-5815.2002, *Applied and Environmental*
43 *Microbiology*, 2002.

44 Yvon, S. A., Cooper, D. J., Koropalov, V., and Saltzman, E. S.: Atmospheric hydrogen sulfide over the equatorial
45 Pacific (SAGA 3), *Journal of Geophysical Research: Atmospheres*, 98, 16979-16983, 10.1029/92jd00451, 1993.

46 Zhou, X., and Mopper, K.: Photochemical production of low-molecular-weight carbonyl compounds in seawater
47 and surface microlayer and their air-sea exchange, *Marine Chemistry*, 56, 201-213,
48 [https://doi.org/10.1016/S0304-4203\(96\)00076-X](https://doi.org/10.1016/S0304-4203(96)00076-X), 1997.

49

50

51



1

2 **Table 1. Results of the DMS bag sample intercomparison study undertaken during the SOAP voyage. Note that a 1 s**
 3 **PTR-MS dwell time for m/z 63 and 66 was used during the intercomparison compared to the 10 s during ambient**
 4 **measurements; as such the PTR-MS std dev reported here is expected to be ~3 times higher than during ambient**
 5 **measurements. Total refers to the ambient DMS + spiked tri-deuterated DMS bag sample on DOY 65.**

DOY	Comparison	DMS (ppt) av ± stdev			DMS ratios		
		GC-SCD	PTR-MS	mesoCIMS	GC-SCD /PTR-MS	PTR-MS /mesoCIMS	GC-SCD /mesoCIMS
64	<i>Standard (dry)</i>	354 ± 6	339 ± 64	n/a	1.04 ± 0.2	n/a	n/a
65	<i>Standard (dry)</i>	289 ± 2	262 ± 43	383 ± 30	1.1 ± 0.18	0.68 ± 0.12	0.75 ± 0.06
64	<i>Ambient</i>	168 ± 5	158 ± 49	n/a	1.06 ± 0.33	n/a	n/a
65	<i>Ambient</i>	n/a	127 ± 43	141 ± 5	n/a	0.90 ± 0.30	n/a
	<i>+tri-deuterated DMS</i>	n/a	197 ± 49	260 ± 2	n/a	0.76 ± 0.19	n/a
	<i>Total</i>	323 ± 9	324 ± 66	401 ± 6	1.0 ± 0.2	0.81 ± 0.16	0.81 ± 0.03

6

7 **Table 2. MeSH_a, DMS_a and acetone_a measured with PTR-MS during the SOAP voyage, reaction rate constant for OH**
 8 **and calculated lifetime with respect to OH**

9

	Mean (range) ppt	kOH [*] (cm ³ molecule ⁻¹ s ⁻¹)	Lifetime (days)
MeSH	18 (BDL – 65)	3.40E ⁻¹¹	0.4
DMS	208 (BDL – 957)	1.29E ⁻¹¹	1
acetone	237 (54–1508)	2.20E ⁻¹³	60

10

11 BDL= below detection limit

12 ^{*}Reaction rate constants from Atkinson 1997 (MeSH), Berresheim et al 1987 (DMS) and Atkinson 1986 (acetone)

13 **Table 3. Pearson correlations between DMS_a and MeSH_a and acetone_a which are significant at 95% CI. Land influenced**
 14 **data removed (acetone)**

		Slope (p-value)	R ²
DMS vs MeSH	All data (n=266)	0.07 (<0.0001)	0.3
	B2 (n=98)	0.13 (<0.0001)	0.5
	B3 (n=76)	0.03 (0.001)	0.1
DMS vs acetone	All data (n=1301)	0.30 (<0.0001)	0.1
	B1 (n=883)	0.19 (<0.0001)	0.1
	B2 (n=122)	1.1 (<0.0001)	0.2
Acetone vs MeSH	All data (n=265)	0.02 (<0.0001)	0.1
	B3 (n=76)	0.06 (0.03)	0.1



1

2 **Table 4. MeSH and DMS fluxes calculated using the nocturnal buildup method, compared with DMS flux measured**
3 **using EC method (Bell et al., 2015). The \pm values on the MeSH and DMS flux are due to the std deviation of the MBL**
4 **height.**

Bloom	DOY	MeSH ppt/hr	DMS ppt/hr	MeSH/ MeSH+DMS (%)	Flux MeSH $\mu\text{mol}/\text{m}^2/\text{day}$	<u>NBL</u> Flux DMS $\mu\text{mol}/\text{m}^2/\text{day}$	EC Flux DMS mean \pm std dev
Just prior to B2	52.2 - 52.7	3	11	24	3.5 ± 2.0	12.7 ± 7.4	7.6 ± 4.8
B2	54.2 - 54.4	5	16	23	5.8 ± 3.4	18.5 ± 10.7	26.4 ± 9.7
B3a	60.2 - 60.4	4	27	14	4.8 ± 2.8	31.0 ± 17.9	29.4 ± 8.2

5

6

7 **Table 5. MeSH flux from this and previous studies (voyage averages)**

Location	MeSH flux ($\mu\text{mol}/\text{m}^2/\text{day}$)	Flux MeSH/MeSH+DMS (%)	Reference
Baltic sea	0.2	5%	Leck and Rodhe., 1991
Kattegat sea	0.8	4%	
North Sea	1.6	11%	
North/South Atlantic	1.2	16%	Kettle et al., 2001
Northeast subarctic Pacific	Not reported	~15%	Kiene et al., 2017
South West Pacific	4.7	20%	This study

8

9

10

11 **Table 6. Spearman rank correlations significant at 95% confidence interval (CI). Correlation coefficient (and p-value)**
12 **are shown. No entry indicates there was no correlation at 95% CI.**

	Acetone _a	DMS _a	MeSH _a
Positive correlations			
salinity	0.55 (0.005) n=25		
sea temperature	0.77 (<0.0001) n=25		
beta -660 backscatter	0.67 (0.0004) n=25		
TpCO ₂	0.59 (0.029) n=15		
DMS _{sw} (nM)	0.49 (0.025) n=21	0.73(0.0002) n=22	0.59 (0.011) n=18
Chla/MLD	0.50 (0.014) n=25		
particulate nitrogen		0.79 (0.048) n=7	
Cryptophyte algae	0.47 (0.019) n=25		



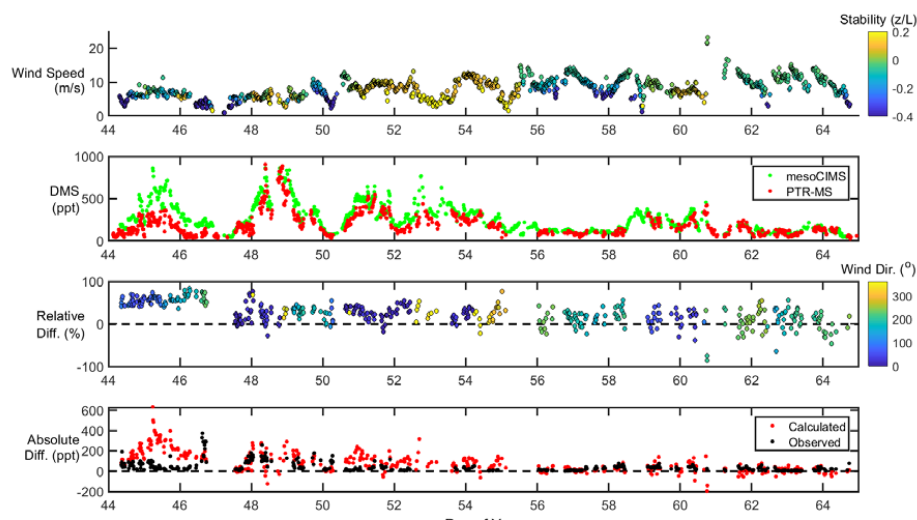
Eukaryotic Picoplankton	0.48 (0.016) n=25		
DMSPt		0.54 (0.011) n=22	0.59 (0.014) n=17
DMSPp		0.56 (0.007) n=22	0.53 (0.032) n=17
CDOM	0.48 (0.041) n=20		
HMW reducing sugars	0.67 (0.011) n=14		
Negative correlations			
Chla/backscatter 660	-0.47 (0.019) n=25		
mixed layer depth	-0.66 (0.0005) n=25		
dissolved oxygen	-0.45 (0.030) n=24		
Phosphate	-0.54 (0.006) n=25		
Nitrate	-0.60 (0.002) n=25		
Silicate	-0.50 (0.012) n=25	-0.43 (0.031) n=26	
Monounsaturated fatty acids	-0.82 (0.007) n=10		

1

2



1
2
3
4



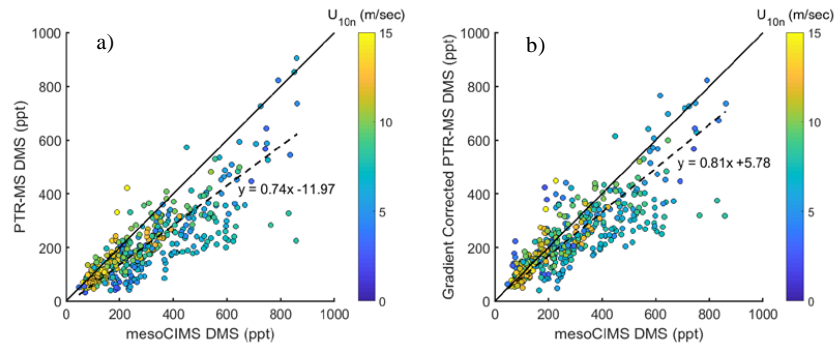
5

6 **Figure 1** From top to bottom, wind speed and stability, DMS_a measurements from mesoCIMS and PTR-MS, relative
7 difference (normalised to mesoCIMS) according to absolute wind direction, and absolute observed and calculated
8 difference between mesoCIMS and PTR-MS, taking into account the expected DMS concentration gradient (Eq. 1)

9



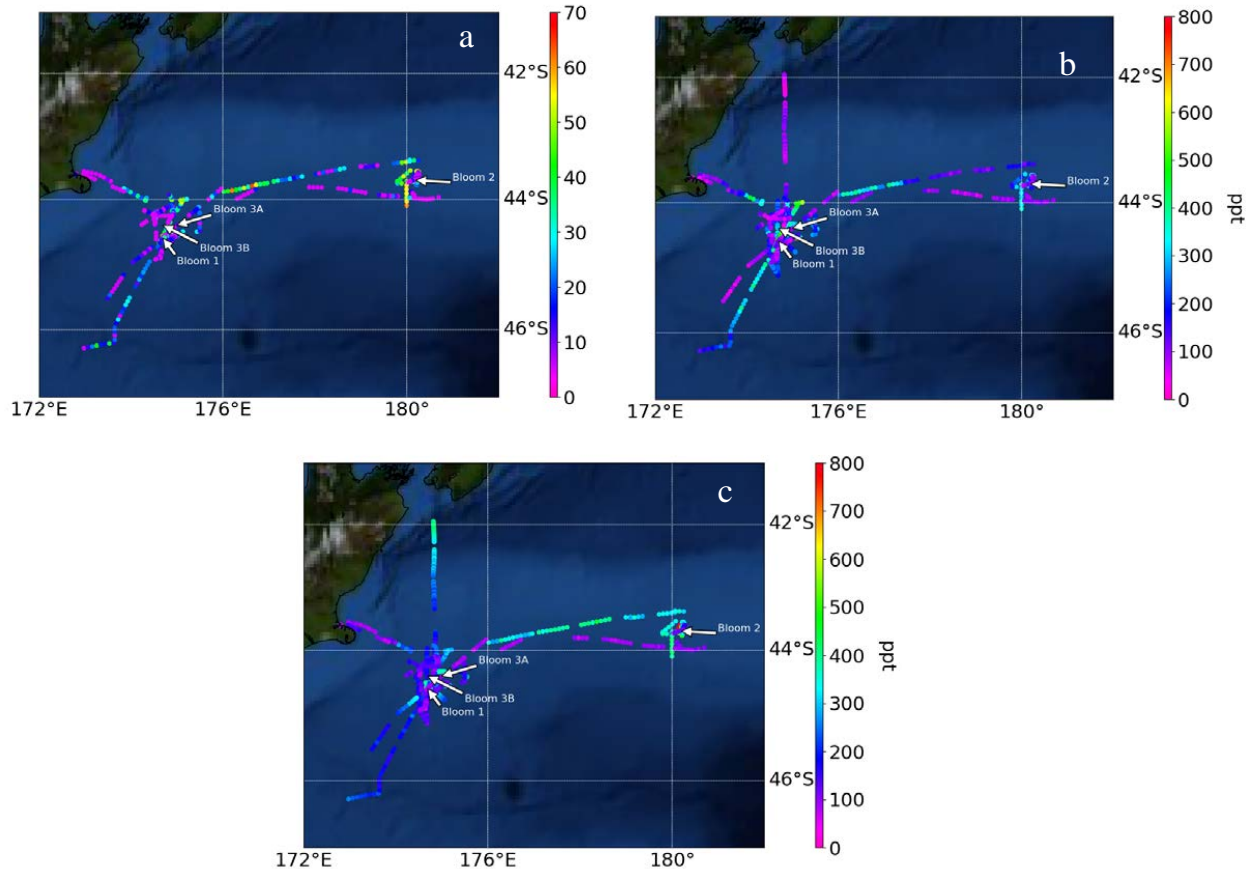
1



2

3 **Fig 2 a) DMSa measured by mesoCIMS (x) and PTR-MS (y) b) mesoCIMS (x) and PTR-MS (y) DMS data corrected
4 for the expected concentration gradient (observed PTR-MS DMS + calculated delta DMS)**

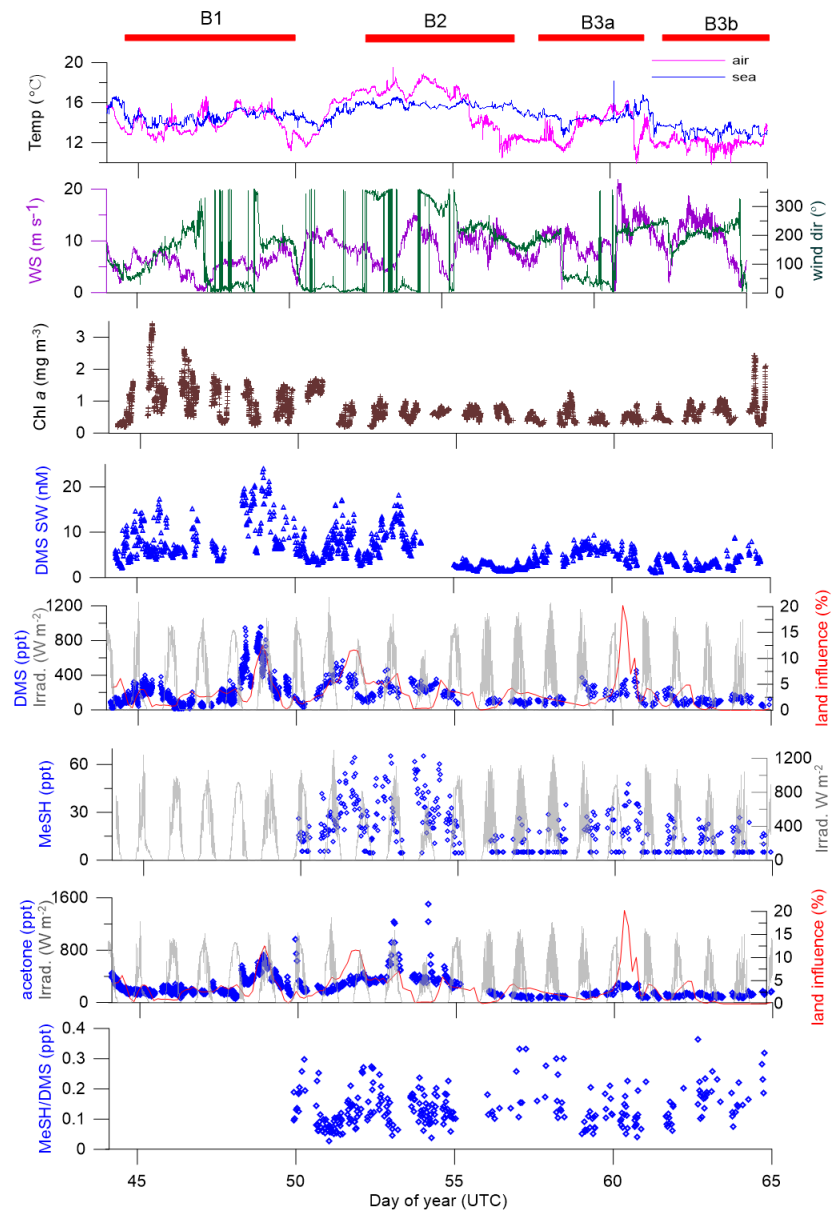
5
6
7
8



1

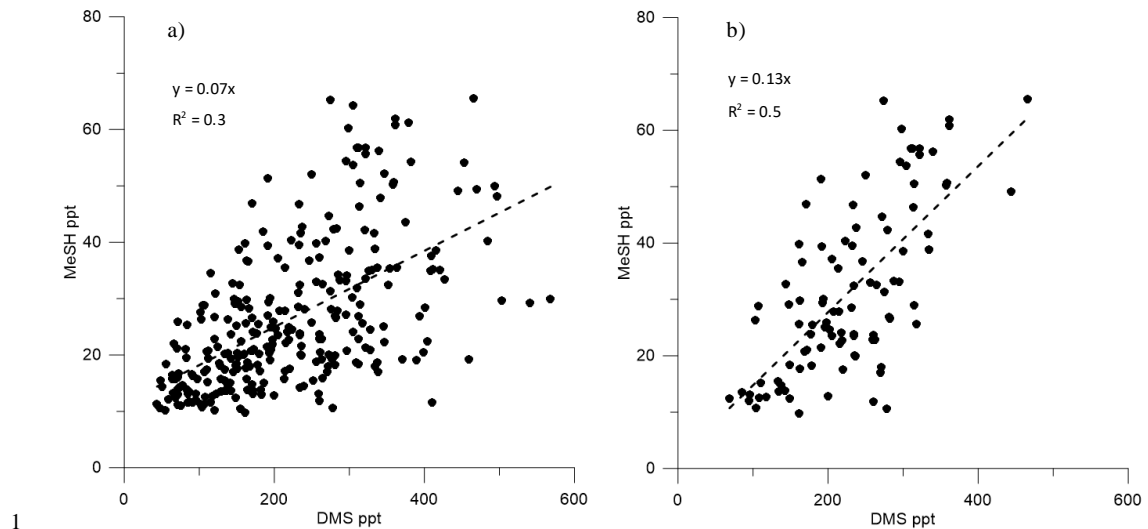
2 **Fig 3 Atmospheric mixing ratios of (a)MeSHa, (b) DMSa and c) acetonea as function of the voyage track. Location of**
3 **the blooms are shown.**

4



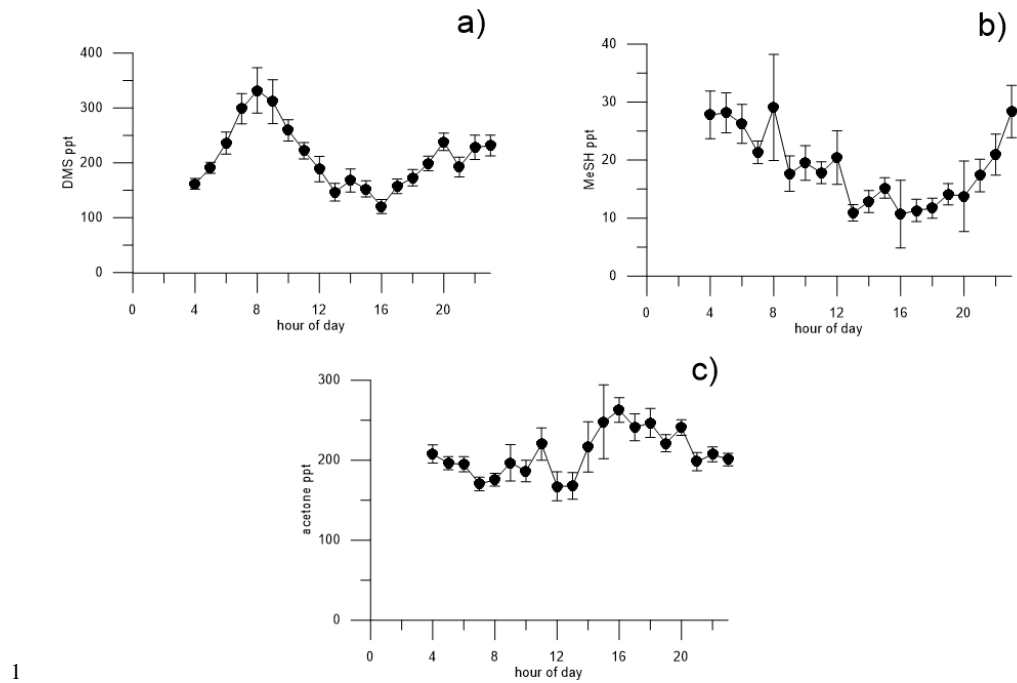
1
2 **Figure 4** -times series of measurements during the SOAP voyage according to DOY. Atmospheric DMS and MeSH
3 measurements below detection limit have had half detection limit substituted.

4



1
2 **Fig 5. Correlation between a) DMS_a and MeSH_a all data (DOY 49 onwards), b) DMS_a and MeSH_a bloom (B2) only**

3



1 **Fig 6. Diurnal cycles of a) DMS, b) MeSH, c) acetone with land influenced data removed. Average values from 0:00-
2 3:00 are excluded because of lower data collection during this period, due to calibrations and zero air measurements**
3
4
5
6
7
8